Journal of Advanced Research 41 (2022) 63–75

Contents lists available at ScienceDirect

Journal of Advanced Research

journal homepage: www.elsevier.com/locate/jare

Original Article

Mechanical overloading induces GPX4-regulated chondrocyte ferroptosis in osteoarthritis via Piezo1 channel facilitated calcium influx

Shaoyi Wang [a,b,c,d,1], Weiwei Li [e,1], Pengfei Zhang [a,f], Zihao Wang [b,f], Xiaoyuan Ma [a], Chuanju Liu [g], Krasimir Vasilev [h,i], Lei Zhang [j], Xiaocong Zhou [k], Liang Liu [l], John Hayball [l,m], Shuli Dong [n], Yuhua Li [a], Yuan Gao [a], Lei Cheng [a,b,*], Yunpeng Zhao [a,*]

[a] Department of Orthopaedic Surgery, Qilu Hospital, Cheeloo College of Medicine, Shandong University, Jinan, Shandong 250012, PR China
[b] Qilu Hospital of Shandong University Spine and Spinal Cord Disease Research Center-ICMRS Collaborating Center for Orthopaedic translational Research, Shandong University, Jinan, Shandong 250012, PR China
[c] Institute of Stomatology, Shandong University, Jinan, Shandong, 250012, PR China
[d] NHC Key Laboratory of Otorhinolaryngology, Qilu Hospital, Cheeloo College of Medicine, Shandong University, Jinan, Shandong 250012, PR China
[e] Department of Pathology, Qilu Hospital, Cheeloo College of Medicine, Shandong University, Jinan, Shandong 250012, PR China
[f] Cheeloo College of Medicine, Shandong University, Jinan, Shandong, 250012, PR China
[g] Department of Orthopaedic Surgery, New York University School of Medicine, New York University Medical Center, New York City, NY, USA
[h] Future Industries Institute, University of South Australia, Mawson Lakes Campus, Mawson Lakes 5095, Australia
[i] School of Engineering, University of South Australia, Mawson Lakes Campus, Mawson Lakes 5095, Australia
[j] Department of Orthopaedic Surgery, The First Affiliated Hospital of Shandong First Medical University, Jinan, Shandong 250012, PR China
[k] Health Management Centre. The First Affiliated Hospital of Shandong First Medical University, Jinan, Shandong 250012, PR China
[l] Experimental Therapeutics Laboratory, University of South Australia Cancer Research Institute, Adelaide SA 5000, Australia
[m] Robinson Research Institute and Adelaide Medical School, University of Adelaide, Adelaide SA 5005, Australia
[n] Key Laboratory of Colloid and Interface Chemistry (Shandong University), Ministry of Education, Jinan 250100, PR China

HIGHLIGHTS

- Our study proved that mechanical overloading induces ferroptosis of chondrocyte, which might be a potential therapeutic target for mechanical damage of chondrocyte and OA.
- Our study demonstrated Piezo1 facilitated calcium influx leads to reduction of GSH, decrease of Gpx4 and activation of oxidative stress in chondrocyte under high strain mechanical stimulation.
- Mechanical signals were converted into ferroptosis-associated signals through Piezo1 channel induced calcium influx, which might shed light on therapeutic interventions for treatment of OA and other diseases associated with ferroptosis.

GRAPHICAL ABSTRACT

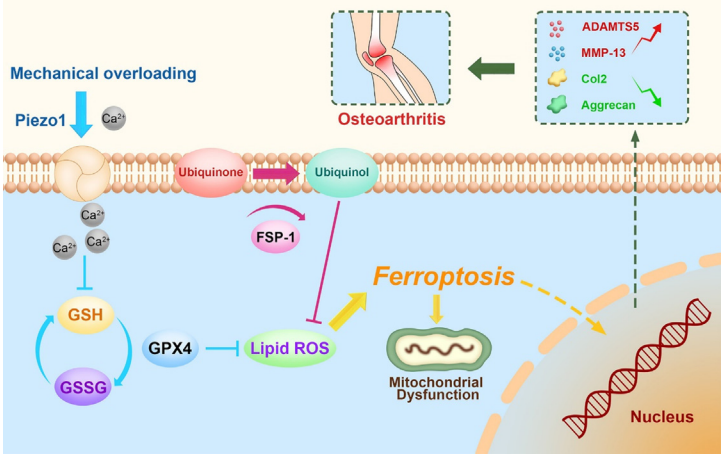

Abbreviations: GPX4, Glutathione peroxidase 4; OA, osteoarthritis; CoQ10, coenzyme Q10; FSP-1, ferroptosis suppressor protein 1; GSH, glutathione; DMM, Destabilization of the medial meniscus; MMP-13, Matrix metallopeptidase 13; ADAMTS-5, A disintegrin and metalloproteinase with thrombospondin motifs-5; Col2, Collagen II; ROS, Reactive oxygen species; GAG, Glycosaminoglycan; OARSI, Osteoarthritis Research Society International.

Peer review under responsibility of Cairo University.

* Corresponding authors at: Qilu Hospital, Cheeloo College of Medicine, Shandong University, 107 Wenhuaxi Road, Jinan, PR China.
E-mail addresses: chenglei@email.sdu.edu.cn (L. Cheng), lwwzyp@email.sdu.edu.cn (Y. Zhao).

[1] These authors contributed equally to this work.

https://doi.org/10.1016/j.jare.2022.01.004
2090-1232/

ARTICLE INFO

Article history:
Received 3 October 2021
Revised 19 December 2021
Accepted 7 January 2022
Available online 11 January 2022

Keywords:
Chondrocytes
Osteoarthritis
Ferroptosis
Mechanical stress
Piezo1

ABSTRACT

Introductions: Excessive mechanical stress is closely associated with cell death in various conditions. Exposure of chondrocytes to excessive mechanical loading leads to a catabolic response as well as exaggerated cell death. Ferroptosis is a recently identified form of cell death during cell aging and degeneration. However, it's potential association with mechanical stress remains to be illustrated.
Objectives: To identify whether excessive mechanical stress can cause ferroptosis. To explore the role of mechanical overloading in chondrocyte ferroptosis.
Methods: Chondrocytes were collected from loading and unloading zones of cartilage in patients with osteoarthritis (OA), and the ferroptosis phenotype was analyzed through transmission electron microscope and microarray. Moreover, the relationship between ferroptosis and OA was analyzed by GPX4-conditional knockout (Col2a1-CreERT: $GPX4^{flox/flox}$) mice OA model and chondrocytes cultured with high strain mechanical stress. Furthermore, the role of Piezo1 ion channel in chondrocyte ferroptosis and OA development was explored by using its inhibitor (GsMTx4) and agonist (Yoda1). Additionally, chondrocyte was cultured in calcium-free medium with mechanical stress, and ferroptosis phenotype was tested.
Results: Human cartilage and mouse chondrocyte experiments revealed that mechanical overloading can induce GPX4-associated ferroptosis. Conditional knockout of GPX4 in cartilage aggravated experimental OA process, while additional treatment with ferroptosis suppressor protein (FSP-1) and coenzyme Q10 (CoQ10) abated OA development in GPX4-CKO mice. In mouse OA model and chondrocyte experiments, inhibition of Piezo1 channel activity increased GPX4 expression, attenuated ferroptosis phenotype and reduced the severity of osteoarthritis. Additionally, high strain mechanical stress induced ferroptosis damage in chondrocyte was largely abolished by blocking calcium influx through calcium-free medium.
Conclusions: Our findings show that mechanical overloading induces ferroptosis through Piezo1 activation and subsequent calcium influx in chondrocytes, which might provide a potential target for OA treatment.

Introduction

Mechanical stimuli, especially high strain mechanical stress, are deeply involved in traumatic events in various cell types [1-6]. Exposure of chondrocytes to excessive mechanical loading leads to a catabolic response and substantial cell death and is closely associated with the pathogenesis of osteoarthritis (OA) [7]. OA is the most prevalent type of arthritis and is mainly characterized by chondrocyte aging [8,9]. As a progressive, degenerative joint disease, OA is the most common cause of disability in adults, yet the factors that induce OA and its underlying mechanisms remain largely unknown.

Cell death, especially programmed cell death, is closely associated with the aging process, in which ferroptosis plays a critical role [10]. Ferroptosis is a recently identified form of necrotic cell death characterized by oxidative damage to phospholipids, which is involved in various conditions [11]. The phospholipid hydroperoxide-reducing enzyme glutathione peroxidase 4 (GPX4) plays a predominant role in regulating ferroptosis [12]. GPX4 production is related to glutathione (GSH) synthesis, which protects cells from ferroptosis [13]. Recently, ferroptosis suppressor protein 1 (Fsp1) has been recognized as a protein that protects against GPX4-associated ferroptosis [14] through a mechanism mediated by coenzyme Q10 (Co-Q10) [15]. To date, ferroptosis regulators, especially GPX4, have been reported to be associated with aging processes, providing potential targets for anti-aging therapy [16,17].

Piezo1, a mechanically sensitive ion channel, has been extensively studied in both physiological and disease processes in organisms [18]. Piezo1 activation leads to cell death [19]. Recent studies have shown that Piezo1 might be involved in cartilage degeneration [20]. As a Ca^{2+}-permeable ion channel, Piezo1 plays a predominant role in mechanical stimulus-induced calcium influx [21] and leads to various biophysical changes in various cell types, including chondrocytes [20,22,23].

In this study, we plan to examine the expression and function of the ferroptosis regulator GPX4 in cartilage and primary chondrocytes during OA development. We will determine the roles of Fsp1 and Co-Q10 in suppressing mechanical stress-induced chondrocyte ferroptosis and cartilage aging following GPX4 deficiency. And, we will investigate the potential involvement and underlying mechanisms of Piezo1 channels in mechanical stimulus-induced chondrocyte ferroptosis and cartilage degeneration.

Results

Excessive stress loading leads to ferroptosis in chondrocytes

Cartilage samples were collected from the loading zone (L) and unloading zone (UL) from patients with OA during total knee arthroplasty to determine the potential involvement of mechanical stress-mediated ferroptosis in OA development. As shown in Fig. 1**A,** intraoperative images indicated remarkable cartilage damage in the loading zone compared with the unloading zone. The X-ray in Fig. 1**B** shows concentrated loading of the loading zone of the knee joint (red arrow). Chondrocytes were collected from each zone, and transmission electron microscopy (TEM) was performed to study alterations in ferroptosis of chondrocytes from the loading zone of OA cartilage. Fig. 1**C** reveals ferroptotic features of mitochondria in chondrocytes from the loading zone, including thickened mitochondrial membranes and shrinkage of mitochondria [24]. We further identified the potential genes involved in overloading-associated OA by collecting mRNA samples from cartilage of each zone and performing microarray assay. Microarray results indicated a decrease in the level of the ferroptosis biomarker GPX4 (red arrow) in chondrocytes in the loading zone compared with the unloading zone, and this trend was consistent with that of aging-associated molecules (Fig. 1**D,** **Figure S1A**). Primary murine chondrocytes were isolated and cultured under 1 MPa of mechanical stress at a frequency of 1 Hz for 1 h to inves-

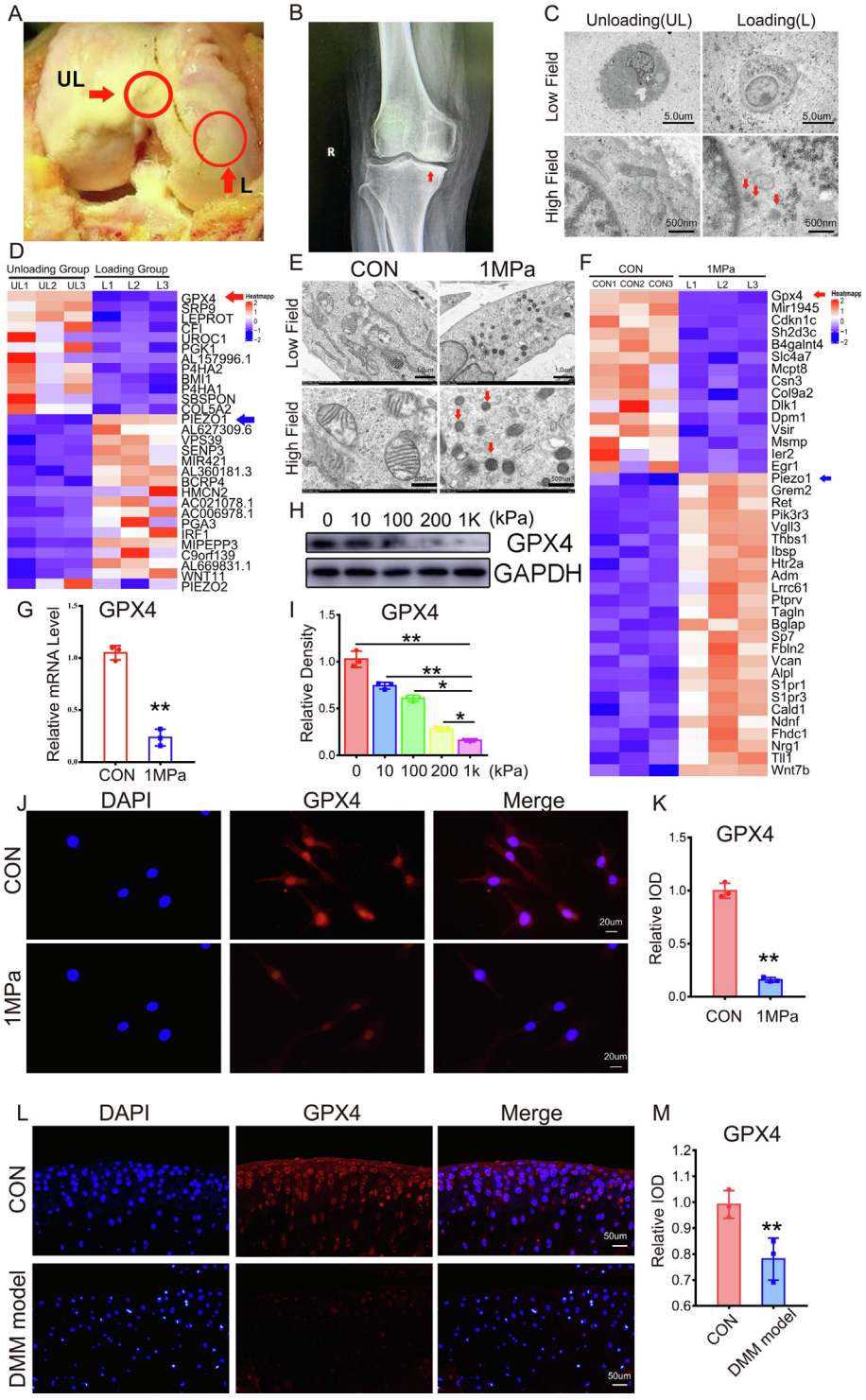

Fig. 1. Excessive stress loading leads to ferroptosis in chondrocytes. (A) The unloading (UL) and loading (L) zone from the articular cartilage of patients with OA. (B) X-ray of the knee joints from patients with OA, and red arrow indicates concentrated loading in the medial part of knee joints. (C) Representative TEM images of chondrocytes from the UL and L zones (n = 3 for each group). Arrows show the shrunken mitochondria. Scale bars, 5 μm (Low field), 500 nm (High field). (D) Microarray heatmap of the indicated groups. (E). Representative TEM images of wild-type mice chondrocytes from the CON group and 1 MPa group (n = 3 for each group). Arrows show the shrunken mitochondria. Scale bars, 1 μm (low field), 500 nm (high field). (F). Microarray heatmap of the indicated groups. (G). Real-time PCR of GPX4 (n = 3 for each group). (H). Western blot (WB) analysis of GPX4 under different pressure conditions. (I). Quantification of WB analysis (n = 3 for each group). (J). Immunofluorescence analysis of GPX4. Scale bars, 20 μm. (K). Quantification of immunofluorescence analysis (n = 3 for each group). (L). Immunofluorescence analysis of GPX4. Scale bars, 50 μm. (M). Quantification of immunofluorescence analysis (n = 3 for each group). Data were presented as the mean ± SD. *P < 0.05, **P < 0.01.

tigate the direct effect of mechanical stimuli on chondrocyte ferroptosis. Thereafter, chondrocytes were cultured for another 24 h, and TEM was performed. As shown in Fig. 1**E**, high strain loading induced ferroptosis-related changes in the mitochondrial structure. Then, mRNA was extracted from each group of chondrocytes following mechanical stimulation, and GPX4 levels (red arrow) were diminished in chondrocytes stimulated with mechanical stress (Fig. 1**F,** **Figure S1D**). Primary murine chondrocytes were cultured with or without overloading, as mentioned above, and mRNA and total protein were extracted and analyzed using real-time PCR and Western blotting, respectively. High strain loading reduced the GPX4 mRNA (Fig. 1**G**) and protein (Fig. 1**H-1I**) levels. Cellular immunofluorescence staining indicated decreased levels of GPX4 in chondrocytes with high strain mechanical loading (Fig. 1**J-1K**). We next examined the localization of GPX4 in articular cartilage from the knee joints of wild-type mice in which a destabilization of the medial meniscus (DMM) model or control model was established. The GPX4 protein was predominantly localized within the superficial zone of cartilage in the normal control group, while GPX4 levels were markedly diminished in cartilage from the DMM model group (Fig. 1**L-1M**).

GPX4-associated ferroptosis exacerbates OA development

Tamoxifen-inducible chondrocyte-specific homozygous GPX4 conditional knockout mice (Col2a1-CreERT, $GPX4^{flox/flox}$) were established by mating Col2a1-CreERT mice with $GPX4^{flox/flox}$ mice to elucidate the physiological roles of endogenous GPX4 in articular cartilage (**Figure S2A**). Col2a1-CreERT $GPX4^{flox/flox}$ (GPX4-CKO) mice developed normally and exhibited no skeletal abnormalities compared with $GPX4^{+/+}$ (wild-type, WT) littermates (Fig. 2**A-2D**). Tamoxifen was administered to 10-week-old GPX4-CKO and WT littermates through intraperitoneal injection once a day for 5 days. Two weeks after the last injection, the specific deletion of GPX4 in cartilage was tested using immunofluorescence staining (Fig. 2**E**), revealing knockout of GPX4 in chondrocytes. Thereafter, the DMM model was established in 12-week-old GPX4- GPX4-CKO and WT mice following the injection of tamoxifen (Fig. 2**F**). Two months after the establishment of the DMM model, the OA phenotype was compared between GPX4-CKO mice and WT mice. As shown in Fig. 2**G-2H**, increased osteophyte formation was detected in the knee joints of CKO mice using the micro-CT assay. Furthermore, safranin-O staining and associated histological analyses were performed, indicating exacerbated development of OA in the GPX4-CKO group (Fig. 2**I-2M**). Immunohistochemical staining also showed decreased expression of anabolic biomarkers, including Aggrecan and collagen 2 (Col2), while the expression of catabolic biomarkers, including Matrix metallopeptidase 13 (MMP13) and A disintegrin and metalloproteinase with thrombospondin motifs-5 (ADAMTS-5), was increased in GPX4-deficient mice (Fig. 2**N-2O**).

The Fsp1-coenzyme Q10 axis is parallel to GPX4-associated ferroptosis and antagonizes ferroptosis in response to GPX4 deficiency [15]. In the present study, Fsp1-AAV or GFP-AAV was delivered into the knee joints of 8-week-old Col2a1-CreERT $GPX4^{flox/flox}$ mice through intraarticular injection (**Figure S3A**). Two weeks later, an IVIS-Spectrum imaging assay was performed, which indicated successful transfection (**Figure S3B**). Cartilage samples were collected, and real-time PCR and cellular immunofluorescence staining for Fsp1 were performed to determine whether the injection increased Fsp1 levels. **Figure S3C** reveals increased Fsp1 mRNA levels in chondrocytes following Fsp1-AAV injection. As shown in **Figure S3D-S3E**, the Fsp1 expression level was markedly increased in chondrocytes following the delivery of Fsp1-AAV. Tamoxifen was subsequently injected into 10-week-old GPX4-CKO mice once a day for 5 days, as indicated in Figure 3A, and a DMM model was established. Two months after surgery, cartilage samples were isolated and micro-CT was performed. As shown in **Figure S3F-S3G**, osteophyte formation was observed in the GFP-AAV control group, which was largely abolished in the Fsp1-AAV infection group. The histological analysis revealed that Fsp1-AAV delivery attenuated cartilage damage and Osteoarthritis Research Society International (OARSI) scores in the GPX4-CKO DMM model (**Figure S3H-S3I**). Immunohistochemistry of articular cartilage indicated that Fsp1 treatment retained anabolic biomarker expression and repressed the expression of catabolic molecules in chondrocytes from GPX4-CKO mice subjected to DMM (**Figure S3J-S3K**).

The DMM model was established in GPX4-CKO mice that were subsequently treated with or without 0.1 g/kg*d Co-Q10 through gastric lavage once a day for two months to investigate the role of Co-Q10 in GPX4-associated chondrocyte ferroptosis and articular cartilage aging (**Figure S3L**). Next, knee joint samples were collected and micro-CT was performed. Osteophyte formation in the DMM model of GPX4-CKO mice was alleviated by additional treatment with Co-Q10 (**Figure S3M-S3N**). Moreover, histology showed that Co-Q10 protected against cartilage degeneration and improved the OARSI score in GPX4-CKO mice (**Figure S3O-S3P**). Immunohistochemistry of articular cartilage also indicated that Co-Q10 treatment increased anabolic biomarker expression and repressed the expression of catabolic molecules in GPX4-CKO mice (**Figure S3Q-S3R**).

Femoral head samples were obtained from 3-week-old WT mice and cultured with or without mechanical stress at 1 MPa with a frequency of 1 Hz for 1 h for ex vivo experiments to further study the direct effect of Co-Q10 on mechanical stimulus-induced cartilage degeneration. The release of proteoglycans into the medium was assayed, and Co-Q10 treatment prevented the release of proteoglycans (**Figure S4A**). In addition, real-time PCR indicated that Co-Q10 treatment increased anabolism and suppressed catabolism in the cultured femoral head cartilage (**Figure S4B-S4E**). Western blot results (**Figure S4F-S4J**) were consistent with the real-time PCR results.

Mechanical overloading induced ferroptosis in chondrocytes through the Piezo 1 ion channel

Increased calcium influx impairs glutathione (GSH) production, which inhibits the function of GPX4 and leads to the destruction of mitochondria [25]. The Piezo1 ion channel is activated by mechanical loading, which facilitates calcium influx under various conditions [22,26]. In the present study, microarray assay results indicated increased Piezo1 levels in the loading zone of articular cartilage from patients with OA (**Figure S1A**, blue arrow) and primary chondrocytes stimulated with mechanical overloading (**Figure S1D**, blue arrow), which was negatively associated with GPX4. Intriguingly, an obvious change in Piezo2 expression was not observed compared with Piezo1 in the loading zone of cartilage and mechanical stimulus-induced chondrocytes based on the microarray assay (**Figure S1**). This information prompted us to determine whether the Piezo1 channel is involved in mechanical overload-induced ferroptosis. Primary WT mouse chondrocytes were cultured under high strain mechanical loading with or without treatment with the Piezo1 inhibitor GsMTx4, followed by staining with Fluo-4 AM Mechanical stimuli induced calcium influx (Fig. 3**A-3B**), while additional treatment with GsMTx4 alleviated this alteration. A live/dead cell assay was also performed, and the results indicated that suppression of the Piezo1 channel by GsMTx4 reduced mechanical stimulus-induced cell death (Fig. 3**-C-3D**). Mechanical overloading also reduced the expression of GSH (Fig. 3**E**), and induced ferroptotic damage in mitochondria (Fig. 3**F**), changes that were attenuated by additional treatment

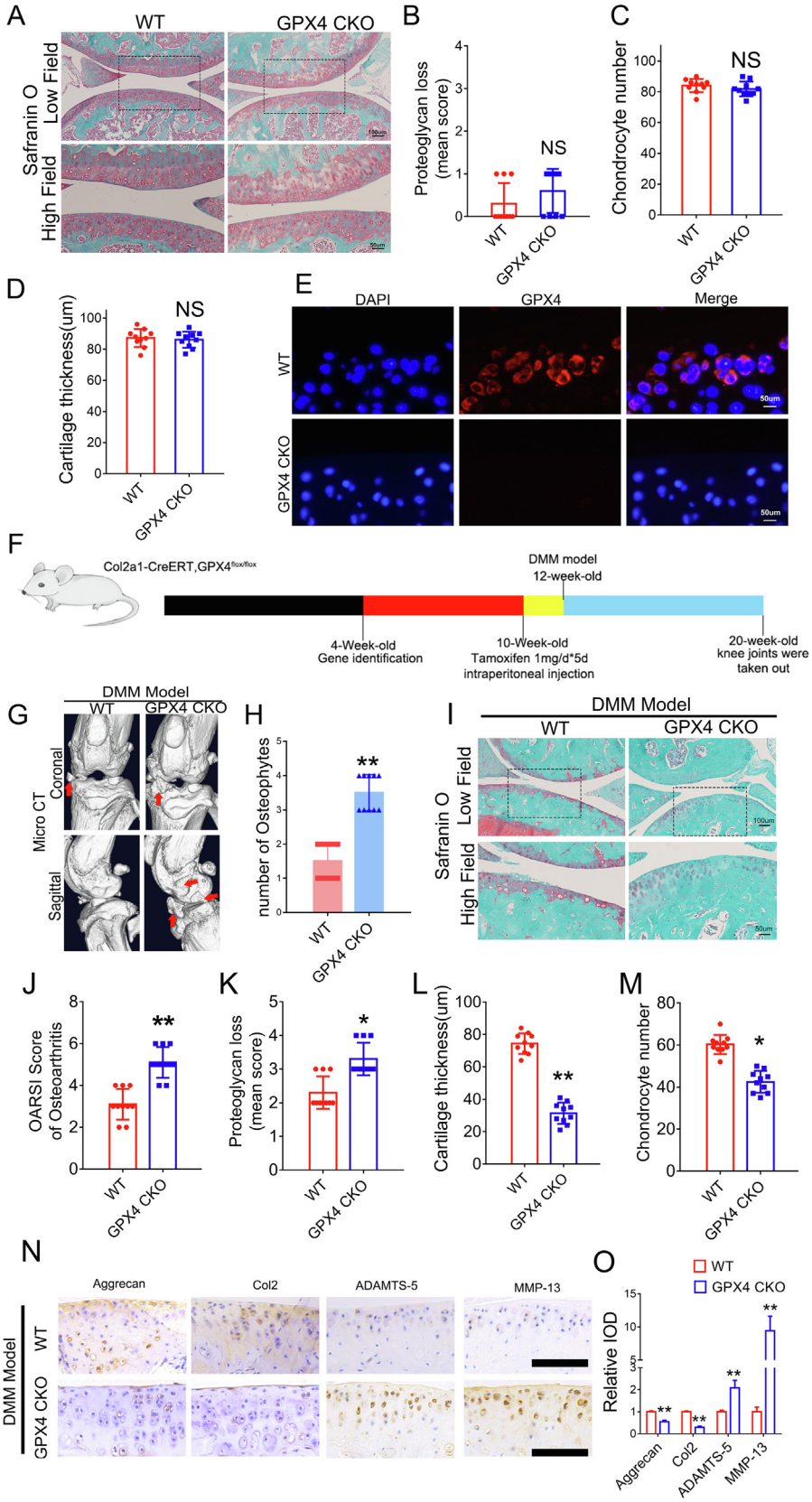

Fig. 2. GPX4-associated ferroptosis exacerbates OA development. (A). Representative images of safranin O staining of cartilage in 12-week-old GPX4 CKO (Col2a1-CreERT, GPX4$^{flox/flox}$) mice and Wild type (WT, GPX4$^{+/+}$) littermates. Scale bars, 100 μm (low field), 50 μm (high field). (B-D). Evaluation of proteoglycan loss, cartilage thickness and chondrocyte number in articular cartilage based on safranin O staining (n = 10 for each group). (E). Immunofluorescence of GPX4. Scale bars, 50 μm. (F). Flowchart of animal experiment. (G). Representative images of Micro-CT of GPX4 CKO mice and WT littermates after DMM model (n = 10 for each group). Arrows show the formation of osteophytes. (H). Osteophyte number assay based on Micro-CT (n = 10 for each group). (I). Representative images of safranin O staining. Scale bars, 100 μm (low field), 50 μm (high field). (J-M). Osteoarthritis Research Society International (OARSI) grade, evaluation of proteoglycan loss, cartilage thickness and chondrocyte number based on safranin O staining (n = 10 for each group). (N). Immunohistochemical assay of Aggrecan, Col2, ADAMTS-5 and MMP-13 in articular cartilage of each group. (O). Quantification of immunohistochemical analysis (n = 3 for each group). Scale bars 50 μm. Data were presented as the mean ± SD. *P < 0.05, **P < 0.01.

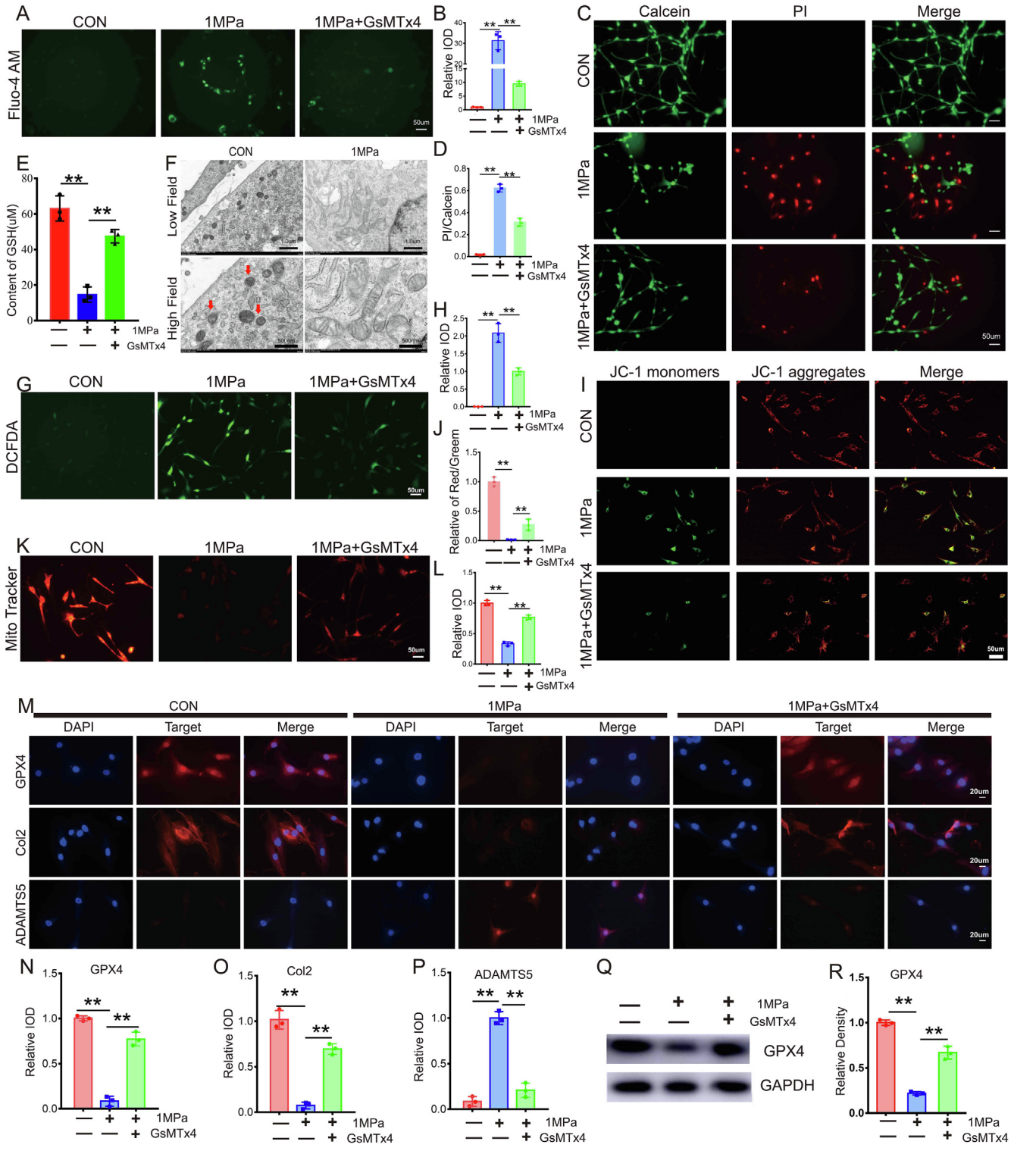

Fig. 3. Mechanical overloading induced ferroptosis in chondrocytes through the Piezo 1 ion channel. (A). Calcium influx was tested by Fluo-4 AM. Scale bar = 50 μm. (B). Quantitative analysis of fluorescence intensity (n = 3 for each group). (C). The cell death ratio of chondrocytes was tested by cell death/live analysis. Scale bar = 50 μm. (D). The cell number of PI (red fluorescence)/calcein (green fluorescence) reflected the cell death ratio (n = 3 for each group). (E). The expression of GSH in chondrocytes was detected by ELISA (n = 3 for each group). (F). Representative TEM images of the indicated groups (n = 3 for each group). Arrows showed shrunken mitochondria. Scale bars, 1 μm (low field), 500 nm (high field). (G). Representative images of ROS levels in chondrocytes. Scale bar = 50 μm. (H). Quantitative analysis of fluorescence intensity (n = 3 for each group). (I). Mitochondrial membrane potential was detected by JC-1 assay. Scale bar = 50 μm. (J). The relative IOD ratio of red fluorescence to green fluorescence was used for quantitative analysis (n = 3 for each group). (K). Representative fluorescence images of mitochondria in chondrocytes. Scale bar = 50 μm. (L). Quantitative analysis of fluorescence intensity (n = 3 for each group). (M). Representative immunofluorescence images of GPX4, Col2 and ADAMTS-5 in chondrocytes. Scale bars 20 μm. (N-P). Quantification of immunofluorescence analysis (n = 3 for each group). (Q). Western blot (WB) analysis of GPX4. (R). Quantification of WB analysis (n = 3 for each group). Data were presented as the mean ± SD. *P < 0.05, **P < 0.01.

with GsMTx4. In the present study, mechanical overloading increased Reactive oxygen species (ROS) production (Fig. 3**G-3H**) and impaired the membrane potential of mitochondria (Fig. 3**I-3J**) in stimulated chondrocytes. MitoTracker staining indicated that the activity of mitochondria [27] in chondrocytes was weakened by mechanical stress (Fig. 3**K-3L**), while suppression of Piezo1 by GsMTx4 reversed these changes in chondrocytes induced by mechanical stimuli. The results of Immunofluorescence staining (Fig. 3**M-3P**) and WB (Fig. 3**Q-3R**) revealed that mechanical overloading reduced GPX4 expression and impaired the metabolism of chondrocytes.

Primary WT mouse chondrocytes were cultured under high strain mechanical stress stimulation with or without the Piezo1 activator Yoda1 to investigate whether the activation of the Piezo1 channel enhances mechanical overload-induced ferroptosis. Then, calcium influx was tested by staining cells with 4-Fluo AM. Yoda1 increased calcium influx in chondrocytes (**Figure S5A-S5B**). A live/dead cell assay was subsequently performed and revealed that the

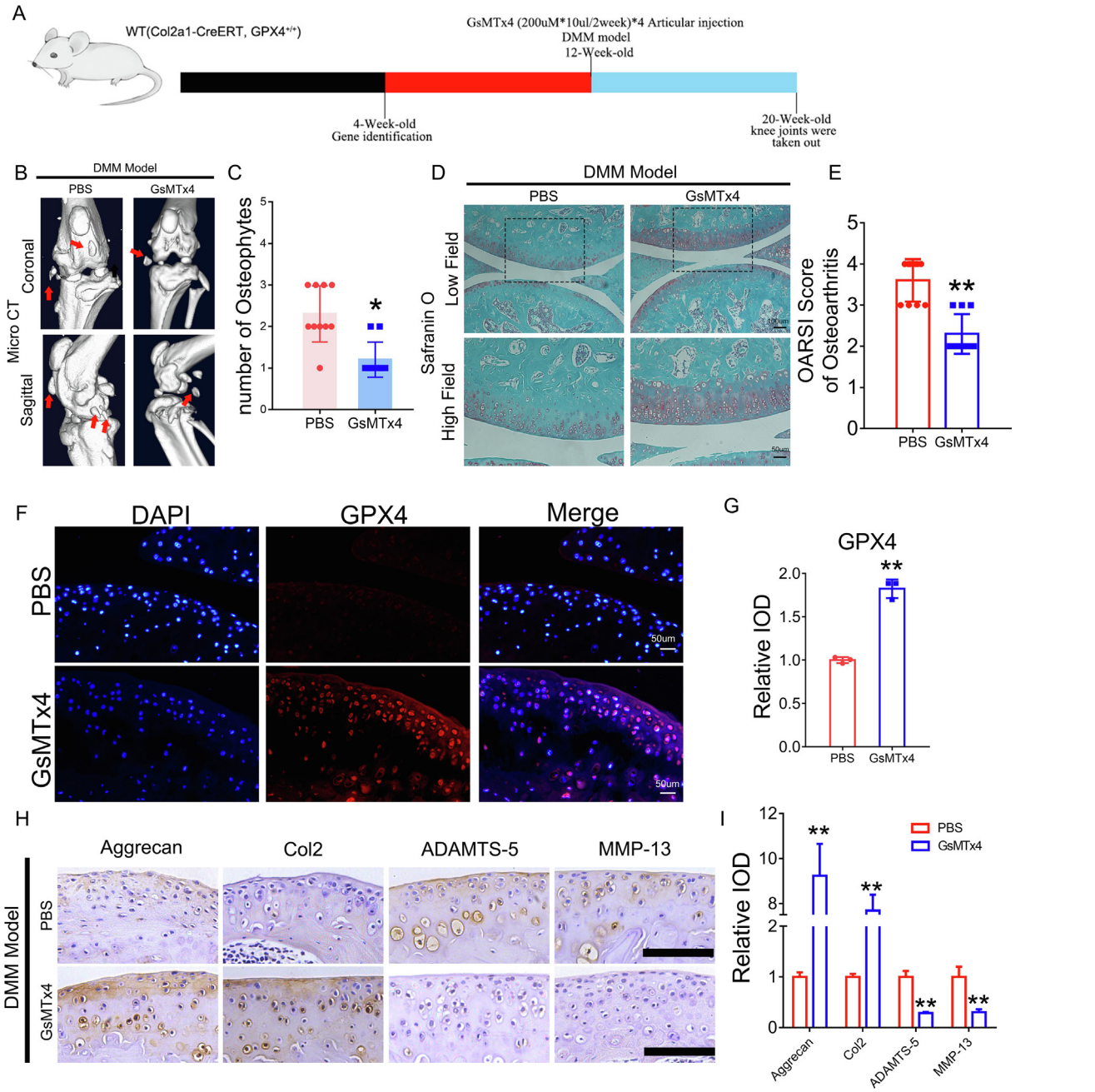

Fig. 4. Suppression of Piezo1 attenuated cartilage aging in a DMM osteoarthritis model. (A). Flowchart of animal experiment. (B). Representative images of Micro-CT of the PBS group and GsMTx4 group after DMM model (n = 10). Arrows show the formation of osteophytes. (C). Osteophyte number assay based on Micro-CT (n = 10 for each group). (D). Representative images of safranin O fast green staining of the PBS group and GsMTx4 group. Scale bars, 100 μm (low field), 50 μm (high field). (E). Osteoarthritis Research Society International (OARSI) score of OA based on the results of safranin O staining (n = 10 for each group). (F). Representative immunofluorescence images of GPX4 in articular cartilage of the indicated group. (G). Quantification of immunofluorescence analysis (n = 3 for each group). (H). Immunohistochemical assay of Aggrecan, Col2, ADAMTS-5 and MMP-13 in articular cartilage of the indicated group. Scale bars 50 μm. (I). Quantification of immunohistochemical analysis (n = 3 for each group). Data were presented as the mean ± SD. *P < 0.05, **P < 0.01.

activation of the Piezo1 channel further increased the percentage of dead chondrocytes stimulated with mechanical overloading (**Figure S5C-S5D**). Next, mRNA and total protein were extracted from each group, and GPX4 levels were analyzed using real-time PCR (**Figure S5E**) and Western blotting (**Figure S5F-S5G**); GPX4 levels were reduced in response to the activation of Piezo1 channels following exposure to mechanical stimuli. DCFDA assays for ROS synthesis (**Figure S5H-S5I**) and JC-1 assays of the mitochon-

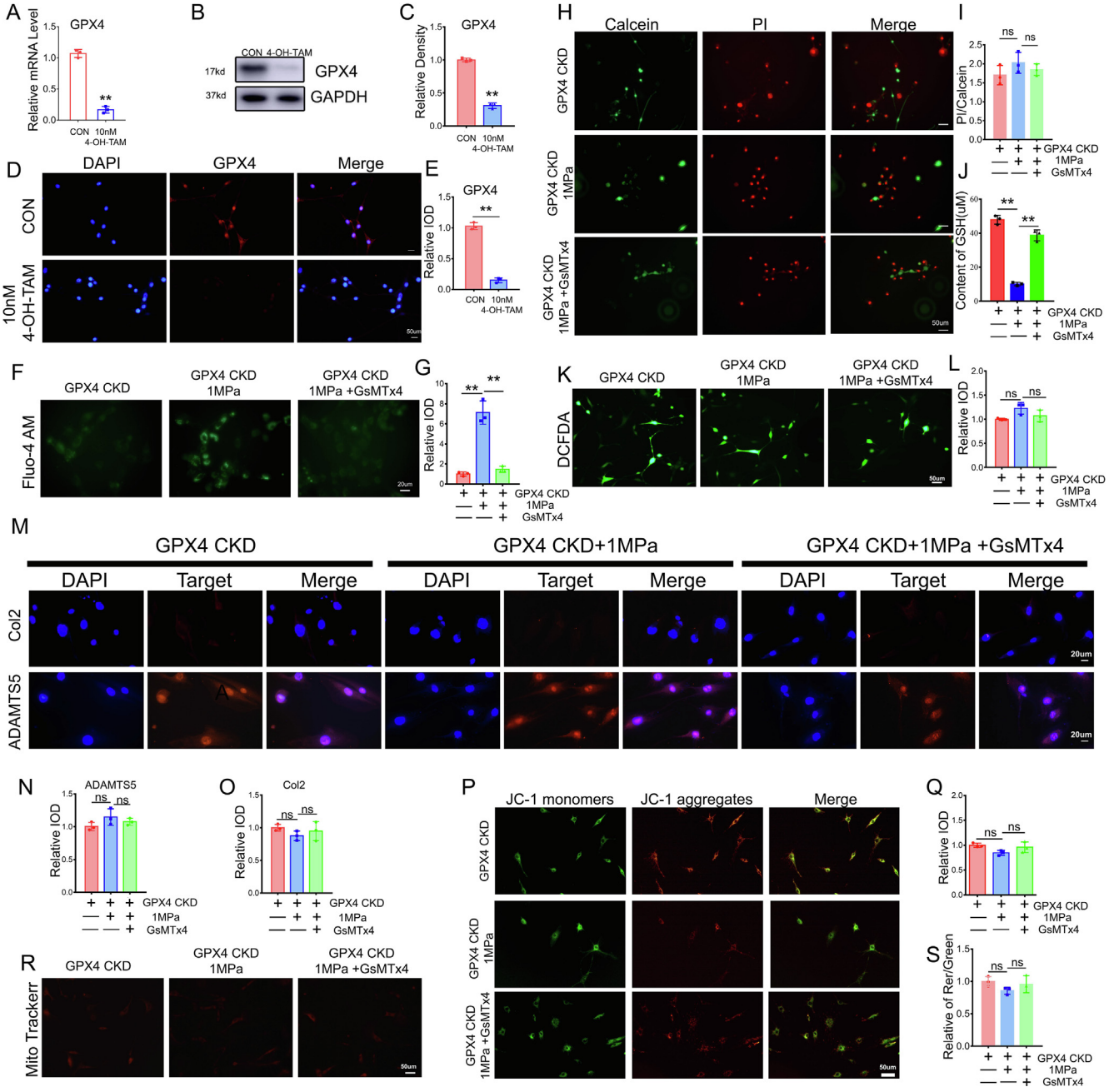

Fig. 5. Suppression of the Piezo1 channel failed to reverse mechanical overload-induced chondrocyte damage in GPX4-deficient mice. (A). Real-time PCR analysis of GPX4 (n = 3 for each group). (B). Western blot (WB) analysis of GPX4. (C). Quantification of WB analysis (n = 3 for each group). (D). Representative immunofluorescence images of GPX4 in chondrocytes. Scale bars 50 μm. (E). Quantification of immunofluorescence analysis (n = 3 for each group). (F). Calcium influx in chromocytes was tested by Fluo-4 AM of chondrocytes in each indicated group. Scale bars 50 μm. (G). Quantitative analysis of fluorescence intensity (n = 3 for each group). (H). Cell death ratio of chondrocytes in each indicated group. Scale bar = 50 μm. (I). The cell number of PI (red fluorescence)/calcein (green fluorescence) reflected the cell death ratio (n = 3 for each group). (J). The expression of GSH in chondrocytes (n = 3 for each group). (K). Representative images of ROS levels in chondrocytes. Scale bar = 50 μm. (L). Quantitative analysis of fluorescence intensity (n = 3 for each group). (M). Representative immunofluorescence images of Col2 and ADAMTS-5 in chondrocytes. Scale bars 20 μm. (N-O). Quantification of immunofluorescence analysis (n = 3 for each group). (P). JC-1 assay of chondrocytes. Scale bar = 50 μm. (Q). The relative IOD ratio of red fluorescence to green fluorescence was used for quantitative analysis (n = 3 for each group). (R). Representative fluorescence images of mitochondria in chondrocytes. Scale bar = 50 μm. (S). Quantitative analysis of fluorescence intensity (n = 3 for each group). Data were presented as the mean ± SD. *P < 0.05, **P < 0.01.

drial membrane potential (**Figure S5J-S5K**) were performed, and activation of Piezo1 by Yoda1 exacerbated the dysfunction of mitochondria in chondrocytes.

Suppression of Piezo1 attenuated cartilage aging in a DMM osteoarthritis model

A DMM model was established in 12-week-old WT mice, and 200 μM*10 μl GsMTx4 or the equivalent amount of PBS was delivered through intraarticular injection twice a week for 8 weeks to determine the role of Piezo1 in OA development (Fig. 4**A**). Joint samples were collected, and micro-CT was performed. As revealed in Fig. 4**B-4C**, osteophyte formation in the knee joint of the DMM model was alleviated by the inactivation of the Piezo1 channel. Safranin-O staining showed that GsMTx4 antagonized cartilage aging and improved the OARSI score in the DMM model (Fig. 4**D-4E**). Immunofluorescence staining for GPX4 was performed to investigate the role of Piezo1 in regulating GPX4 expression during OA development, and the suppression of Piezo1 channel function maintained GPX4 levels in the articular cartilage of the DMM model **(**Fig. 4**F-4G)**. In addition, immunohistochemistry of articular cartilage indicated that GsMTx4 treatment increased the expression of anabolic biomarkers (Aggrecan and Col2) and suppressed the production of catabolic molecules (ADAMTST-5 and MMP-13) in the DMM model (Fig. 4**H-4I**).

Femoral head samples were isolated from 3-week-old WT mice and cultured with mechanical stimulation in the presence or absence of GsMTx4 to further determine the involvement of Piezo1 in chondrocyte metabolism. The release of proteoglycans into the medium was assayed, and GsMTx4 alleviated the loss of proteoglycans in the femoral head (**Figure S6A**). Moreover, real-time PCR indicated that GsMTx4 increased the expression of anabolic biomarkers and suppressed the expression of catabolic molecules in the cultured femoral heads (**Figure S6B-S6E**). Western blotting was also performed, and the results (**Figure S6F-S6J**) were consistent with the real-time PCR results.

Suppression of the Piezo1 channel failed to reverse mechanical overload-induced chondrocyte damage in GPX4-deficient mice

Chondrocytes from 5-day-old Col2a1-CreERT GPX4$^{flox/flox}$ mice were isolated and incubated with 10 nM 4-OH-tamoxifen for 3 days as reported previously to knock down GPX4 and determine the specific interaction between GPX4 and the Piezo1 channel in mechanical overload-induced chondrocyte injury. Real-time PCR (Fig. 5**A**), WB (Fig. 5**B-5C**) and immunofluorescence staining (Fig. 5**D-5E**) confirmed the high efficiency of GPX4 deletion in chondrocytes. The induced chondrocytes were subsequently cultured under high mechanical stress with or without GsMTx4 treatment and stained with Fluo-4 AM. As shown in Fig. 5**F-5G**, mechanical overloading caused calcium influx, while GsMTx4 alleviated this alteration in chondrocytes. However, the live/dead cell assay (Fig. 5**H-5I**) showed no significant difference in cell mortality with or without inhibition of the Piezo1 channel. Intriguingly, mechanical stress still reduced GSH expression (Fig. 5**J**), while GsMTx4 retained the GSH content due to insufficient GPX4 expression. Nevertheless, DCFDA assays for ROS (Fig. 5**K-5L**) showed that suppression of the Piezo1 channel failed to diminish mechanical overload-induced ROS production in mice lacking GPX4. Immunofluorescence staining (Fig. 5**M-5O**) showed that GsMTx4 did not improve chondrocyte metabolism in 4-OH-tamoxifen-induced GPX4-CKO chondrocytes. GPX4 knockdown decreased the protective effect of GsMTx4 on the mechanical overload-mediated impairment in the mitochondrial membrane potential (Fig. 5**P-5Q**) and destruction of mitochondria (Fig. 5**R-5S**).

Calcium influx was required for mechanical stimulus-induced ferroptosis in chondrocytes

Disorganized calcium influx leads to ferroptosis under several conditions [28]. Based on this finding and the result from the present study that mechanical overload-induced ferroptosis in chondrocytes is accompanied by increased influx of calcium ions, we investigated whether calcium ions were required for mechanical overload-induced ferroptosis. In the present study, calcium-free medium was used to remove extracellular calcium ions, and WT murine chondrocytes were cultured. The Fluo-4 AM assay confirmed the lack of obvious calcium influx in chondrocytes cultured with calcium-free medium even after mechanical stimulation (Fig. 6**A-6B**). The increased rate of chondrocyte death caused by mechanical stress was also largely abolished in the absence of calcium influx into chondrocytes (Fig. 6**C-6D**). Interestingly, GSH levels were maintained following the suppression of calcium influx (Fig. 6**E**), consistent with previous findings [28,29]. Furthermore, ROS production was decreased (Fig. 6**F-6G**), mitochondrial destruction was alleviated (Fig. 6**H-6I**), and the mitochondrial membrane potential was maintained (Fig. 6**J-6K**). Real-time PCR (Fig. 6**L**), immunofluorescence (Fig. 6**M-6P**) and WB (Fig. 6**Q-6R**) revealed that the absence of calcium influx largely maintained GPX4 levels, reduced the production of catabolic biomarkers, including ADAMTS-5 and MMP-13, and promoted the secretion of the anabolic biomarker Col2 in response to mechanical overload.

Discussion

OA is a common degenerative disease in the clinic that is mainly characterized by the destruction of articular cartilage [30]. OA is caused by an imbalance of anabolic and catabolic factors, which is strongly associated with abnormal mechanical stress [31]. Mechanical overloading impairs biochemical pathways in chondrocytes, leading to reduced production of extracellular matrix (ECM) and increased degradation of ECM molecules by related proteases in chondrocytes [32].

Based on accumulating evidence, chondrocyte death plays a critical role in OA pathogenesis [33]. Ferroptosis is a recently identified form of pathophysiological cell death that leads to mitochondrial dysfunction and oxidative damage to cells [34]. In the present study, chondrocytes in the loading zone of articular cartilage from patients with OA and mechanical overload-stimulated chondrocytes underwent ferroptosis, consistent with chondrocyte degeneration. This finding suggests the potential involvement of mechanical loading-associated chondrocyte ferroptosis in the cartilage aging process. GPX4 is reportedly a key regulator of ferroptosis and exerts a protective effect on ferroptotic damage in cells under various conditions [13]. GSH homeostasis is accepted to be vital for the normal production and function of GPX4 [35]. In the present study, GPX4 levels were decreased in degenerating chondrocytes, implying a potential association between GPX4 expression and OA development. A DMM mouse model was established in this study, and concentrated mechanical loading in knee joints leads to an OA phenotype in this model [36]. GPX4-CKO mice displayed exacerbated OA development compared with WT littermates, implying that the loss of GPX4 in chondrocytes impaired the normal response of cartilage to mechanical overloading.

The Fsp1-Co-Q10 axis was recently identified as a key regulator of ferroptosis that is parallel to GPX4 and even rescues the ferroptosis phenotype of cells deficient in GPX4 [14,15]. These ferroptosis regulators have been extensively studied for their potential therapeutic effects on several conditions [37,38]. Here, the administration of Fsp1 and Co-Q10 antagonized the OA phenotype of GPX4-CKO mice and exerted a protective effect on mechanical

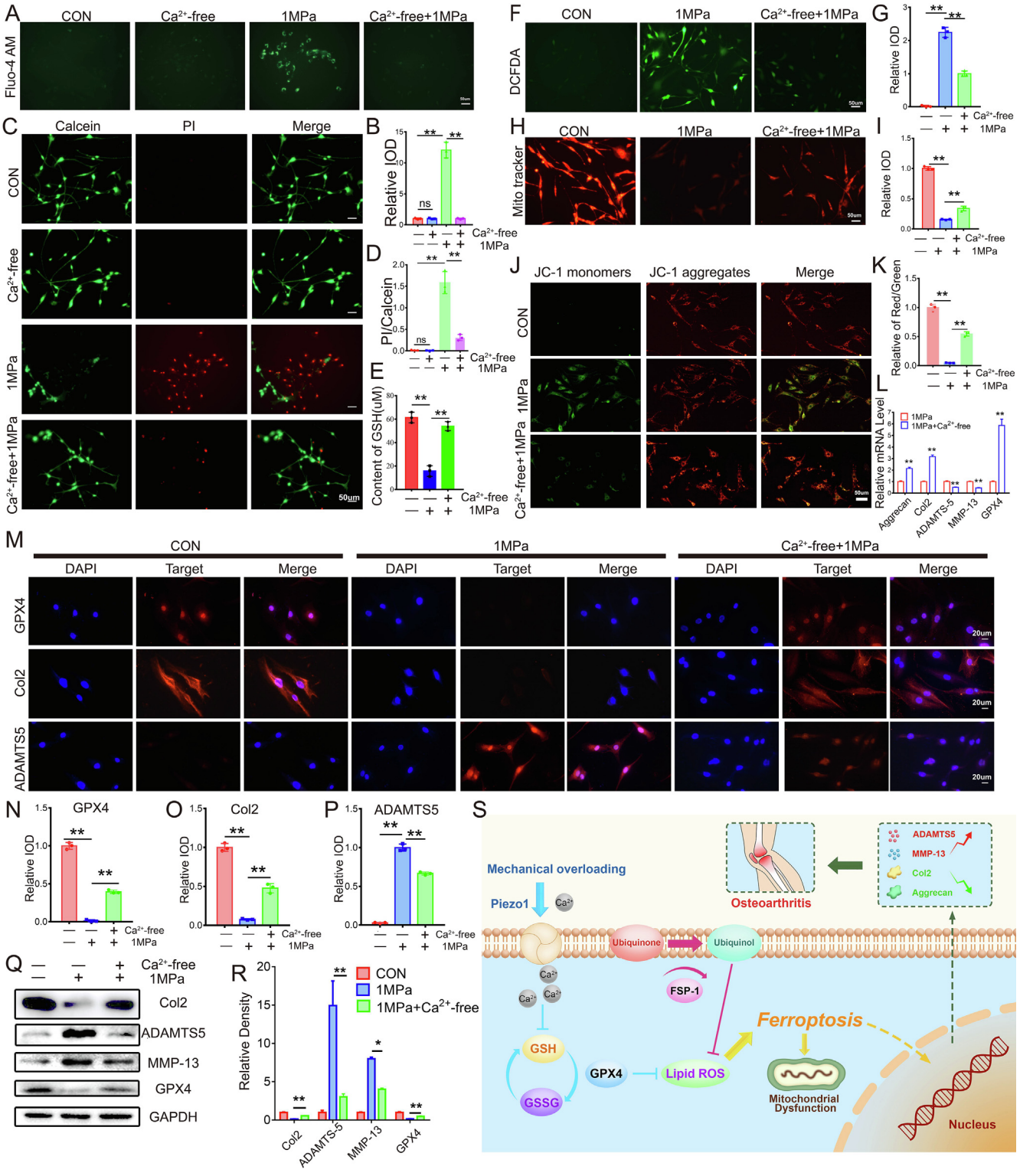

Fig. 6. Calcium influx was required for mechanical stimulus-induced ferroptosis in chondrocytes. (A). Calcium influx in chromocytes was tested by Fluo-4 AM of chondrocytes in each indicated group. Scale bars 50 μm. (B). Quantitative analysis of fluorescence intensity (n = 3 for each group). (C). Cell death ratio of chondrocytes in each indicated group. Scale bar = 50 μm. (D). The cell number of PI (red fluorescence)/calcein (green fluorescence) reflected the cell death ratio (n = 3 for each group). (E). The expression of GSH in chondrocytes (n = 3 for each group). (F). Representative images of ROS levels in chondrocytes in each indicated group. Scale bar = 50 μm. (G). Quantitative analysis of fluorescence intensity (n = 3 for each group). (H). Representative fluorescence images of mitochondria in chondrocytes. Scale bar = 50 μm. (I). Quantitative analysis of fluorescence intensity (n = 3 for each group). (J). JC-1 assay of chondrocytes in each indicated group. Scale bar = 50 μm. (K). The relative IOD ratio of red fluorescence to green fluorescence was used for quantitative analysis (n = 3 for each group). (L). Real-time PCR analysis of GPX4, Aggrecan, Col2, ADAMTS-5 and MMP-13 in chondrocytes (n = 3 for each group). (M). Representative immunofluorescence images of GPX4, Col2 and ADAMTS-5 in chondrocytes. Scale bars 20 μm. (N-P). Quantification of immunofluorescence analysis (n = 3 for each group). (Q). Western blot (WB) analysis of GPX4, Col2, ADAMTS-5 and MMP-13 in chondrocytes. (R). Quantification of WB analysis (n = 3 for each group). (S). Schematic diagram of mechanical overloading induced ferroptosis in chondrocyte. Data were presented as the mean ± SD. *P < 0.05, **P < 0.01.

overload-mediated disruptions in chondrocyte metabolism. Therefore, mechanical overload-induced chondrocyte ferroptosis might be mainly facilitated by an impairment of the GPX4-associated pathway.

Piezo channels are involved in mechanical stimulus-induced alterations in cell viability [39,40]. In the current study, activation of the Piezo1 channel was associated with chondrocyte ferroptosis, leading to impaired GSH function, a reduction in GPX4 expression and ferroptotic damage to mitochondria. According to previous reports, the Piezo1 channel causes metabolic disorders in chondrocytes under mechanical stress [23]. Here, the suppression of Piezo1 by GsMTx4 attenuated OA pathogenesis in a DMM model established in WT mice. Interestingly, GsMTx4 treatment maintained GPX4 levels in articular chondrocytes from the DMM model, consistent with the metabolic alterations. Surprisingly, inhibition of Piezo1 channel function by GsMTx4 failed to rescue mechanical overload-induced chondrocyte injury when GPX4 was genetically suppressed. Thus, GPX4 might be a key downstream target of the Piezo1 channel in mechanical overload-induced chondrocyte ferroptosis.

The Piezo1 channel facilitates calcium influx under mechanical overloading [41]. Moreover, increased influx of calcium ions is reported to trigger cell death [42,43], which exerts a detrimental effect on chondrocyte aging and OA development [44,45]. In the present study, activation of the Piezo1 channel was increased, while inhibition of the Piezo1 channel decreased calcium influx in chondrocytes following mechanical overloading. Intracellular calcium ions are known to interfere with GSH levels in several cell types [28,29]. Here, we detected increased calcium influx in response to mechanical stress stimulation, which in turn reduced GSH and GPX4 levels and led to mitochondrial dysfunction and oxidative stress. Calcium overload is reported to be involved in ferroptotic damage to cells [28,46]. We used calcium-free medium and found that the depletion of calcium influx largely abolished mechanical overload-mediated ferroptotic alterations and oxidative stress in chondrocytes, suggesting the close association of calcium influx with mechanical overload-mediated ferroptotic damage to chondrocytes.

Based on the findings from the current study and various previous studies, a model was proposed to illuminate the underlying mechanism by which mechanical loading induces chondrocyte ferroptosis (Fig. 6**S**). Upon mechanical overloading, the Piezo1 channel is activated and subsequently markedly increases calcium influx. The accumulation of calcium ions in chondrocytes then impairs GSH production, reduces GPX4 levels, and alters ferroptosis in chondrocytes, which are characterized by mitochondrial dysfunction and exacerbated oxidative stress. Intriguingly, the additional supplementation of ferroptosis regulators Fsp1 and Co-Q10 rescues the ferroptosis changes and oxidative damage of chondrocytes exposed to mechanical overloading.

In summary, this study describes the underlying mechanism of mechanical overloading in chondrocytes, during which mechanical stimulation is transferred to the GPX4-associated ferroptosis pathway and causes subsequent chondrocyte aging. This information might provide insights into potential therapeutic interventions for OA and other cartilage degenerative diseases.

Materials and methods

Animals

All animal experiments described in this study were performed in accordance with institutional guidelines and approved by the Laboratory Animal Centre of Qilu Hospital of Shandong University (KYLL-2019(KS)-368). Col2a1-CreERT mice were established by and purchased from Cyagen (USA). $GPX4^{flox/+}$ mice were created by Cyagen (USA) through ES genome engineering. $GPX4^{flox/+}$ mice were mated with $GPX4^{flox/+}$ mice to generate $GPX4^{flox/flox}$ mice. $GPX4^{flox/flox}$ mice were mated with Col2a1-CreERT mice to generate Col2a1-CreERT, $GPX4^{flox/+}$ mice. Col2a1-CreERT $GPX4^{flox/+}$ mice were mated with Col2a1-CreERT $GPX4^{flox/+}$ mice to generate Col2a1-CreERT $GPX4^{flox/flox}$ mice (**Figure S3A**). Male mice with the Col2a1-CreERT and $GPX4^{flox/flox}$ genes were used in experiments. Col2a1-CreERT $GPX4^{+/+}$ littermates were assigned to the wild-type (WT) group [47]. Ten-week-old Col2a1-CreERT $GPX4^{flox/flox}$ mice were intraperitoneally injected with tamoxifen (1 mg/d*5 d) (MCE, USA, Cat#HY-13757A) to obtain GPX4-conditional knockout (GPX4-CKO) mice [47]. C57/BL6 wild-type (WT) mice were purchased from the Experimental Animal Center of Shandong University. Wistar rats were purchased from Vital River Laboratory Animal Technology (Beijing, China). All animals were housed under controlled, identical specific pathogen-free (SPF) standard environmental conditions (23 ± 2 °C, 12-hour light/-dark cycle) with free access to food and water.

Mice were orally administered 0.1 g/kg Co-Q10 daily for 8 weeks after the DMM model was established to investigate the therapeutic effect of Co-Q10 in GPX4-CKO mice with osteoarthritis [48].

Genotyping

Tail clippings were obtained from 4-week-old mice. Mouse tail DNA was extracted using a One Step Mouse Genotyping Kit (Vazyme, China, Cat# PD101-01) according to the manufacturer's instructions. The primers used for amplification (GPX4flox and Col2a1-CreERT) are listed in **Table S1**. Agarose (1.5 g), 100 mL of 2* Tris-acetate-EDTA buffer (TAE) and 6 μl of Gel Red were mixed and heated to form agarose gels. The amplified DNA was subjected to agarose gel electrophoresis. Images were captured using an Amersham Imager 680 (GE, USA). The positive genotype Col2a1-CreERT was a 358 bp band, and no band was detected for the wild-type allele. The $GPX4^{flox/flox}$ alleles were present as a 238 bp band, the wild-type alleles ($GPX4^{+/+}$) were detected as a 204 bp band, and the $GPX4^{flox/+}$ genotype was detected as two bands at 238 and 204 bp. The primers are listed in **Table S1.** The results are listed in **Figure S2B-C**.

Surgically induced OA model

Mice and rats were anaesthetized with pentobarbital. Destabilization of the medial meniscus (DMM) surgery was performed under a microscope [49]. The incision was sutured and disinfected daily until it healed. All mice and rats were housed under normal conditions. Biting incisions were avoided.

Primary cell isolation and culture

Primary mouse chondrocytes were extracted as previously described [50]. Briefly, cartilage tissues from the distal femur and the proximal tibia of 5-day-old mice were harvested under a microscope. The cells were digested with 0.2% collagenase type II (Gibco) at 37 °C for 8 h. Chondrocytes were seeded at a density of 5.7×10^5 cells/cm^2, cultured in DMEM/F12 (HyClone, Logan, USA) supplemented with 10% fetal bovine serum (FBS; Gibco, USA), 100 U/ml penicillin, and 0.1 mg/ml streptomycin (HyClone, USA) and incubated under standard conditions (37 °C, 5% CO2). The culture medium was replaced every 3 days. Chondrocytes were used for up to five generations in all vitro experiments. All experiments were performed with two replicate wells.

Chondrocytes from 5-day-old Col2a1-CreERT $GPX4^{flox/flox}$ mice were collected for in vitro experiments. Chondrocytes were cul-

tured with 10 nM 4-OH-tamoxifen (Apexbio, USA, Cat# B5421) for 3 days to knock down GPX4 [51].

Ethics statement

Patients involved in the study provided consent, and the study was approved based on the medical ethics regulations of the Medical Ethical Committee of Qilu Hospital of Shandong University (KYLI-2020(KS)-624). All animal experiments described in this study were performed in accordance with institutional guidelines and approved by the Laboratory Animal Centre of Qilu Hospital of Shandong University (KYLL-2019(KS)-368).

Statistical analyses

GraphPad Prism 7 software (GraphPad Software Inc., San Diego, CA, USA) was used for statistical analyses of all data. For comparisons between multiple groups, t tests, one-way or two-way ANOVA were performed. The data are presented as the mean values ± standard deviations (SD), and $P < 0.05$ was considered significant. All cell-based experiments were repeated at least three times.

More detailed experimental procedures are described in the online supplementary data: Materials and Methods.

Compliance with ethics requirements

All animal experiments in this study were performed in accordance with institutional guidelines and approved by the Laboratory Animal Centre of Qilu Hospital of Shandong University (KYLL-2019(KS)-368).

Patients involved in the study provided consent, and the study was approved by medical ethics regulations of the Medical Ethical Committee of Qilu Hospital of Shandong University (KYLI-2020(KS)-624).

Declaration of Competing Interest

The authors declare that they have no known competing financial interests or personal relationships that could have appeared to influence the work reported in this paper.

Acknowledgements

This work was supported by National key research and development program of China (Grant No. 2020YFC2009004 to Lei Cheng), National Natural Science Foundation of China (grant No. 81572191 to Lei Cheng, grant No. 81501880 and 82072478 to Yunpeng Zhao, grant No. 81602761 and 82073437 to Weiwei Li), Shandong Provincial Natural Science Foundation (grant No. ZR2020YQ54, ZR019MH05 and ZR201808130091 to Yunpeng Zhao), Cross-disciplinary Fund of Shandong University grant No. 2018JC007 to Yunpeng Zhao), and Shandong Province Key Research and Development Project (grant No. 2019GSF108152 to Yuhua Li).

We thank Translational Medicine Core Facility of Shandong University for consultation and instrument availability that supported this work.

Data availability statement

Data are available in a public, open access repository. All data relevant to the study are included in the article or uploaded as supplementary information.

Appendix A. Supplementary data

Supplementary data to this article can be found online at https://doi.org/10.1016/j.jare.2022.01.004.

References

[1] Lewko B, Stepinski J. Hyperglycemia and mechanical stress: targeting the renal podocyte. J Cell Physiol 2009;221(2):288–95. doi: https://doi.org/10.1002/jcp.21856.
[2] Scott A, Khan K, Heer J, Cook J, Lian O, Duronio V. High strain mechanical loading rapidly induces tendon apoptosis: an ex vivo rat tibialis anterior model. Br J Sports Med 2005;39(5):. doi: https://doi.org/10.1136/bjsm.2004.015164e25.
[3] Nava MM, Miroshnikova YA, Biggs LC, Whitefield DB, Metge F, Boucas J, et al. Heterochromatin-Driven Nuclear Softening Protects the Genome against Mechanical Stress-Induced Damage. Cell 2020;181(4):800–817.e22. doi: https://doi.org/10.1016/j.cell.2020.03.052.
[4] Zhang X, Jing Y, Qin C, Liu C, Yang D, Gao F, et al. Mechanical stress regulates autophagic flux to affect apoptosis after spinal cord injury. J Cell Mol Med 2020;24(21):12765–76. doi: https://doi.org/10.1111/jcmm.15863.
[5] Tang J, Liu C, Li B, Hong S, Li Q, Wang L, et al. Protective Role of Nuclear Factor Erythroid-2-Related Factor 2 against Mechanical Trauma-Induced Apoptosis in a Vaginal Distension-Induced Stress Urinary Incontinence Mouse Model. Oxid Med Cell Longevity 2019;2019:1–10. doi: https://doi.org/10.1155/2019/2039856.
[6] Cabrera-Benítez NE, Parotto M, Post M, Han B, Spieth PM, Cheng W-E, et al. Mechanical stress induces lung fibrosis by epithelial-mesenchymal transition. Crit Care Med 2012;40(2):510–7. doi: https://doi.org/10.1097/CCM.0b013e31822f09d7.
[7] Argote PF, Kaplan JT, Poon A, Xu X, Cai L, Emery NC, et al. Chondrocyte viability is lost during high-rate impact loading by transfer of amplified strain, but not stress, to pericellular and cellular regions. Osteoarthritis Cartilage 2019;27(12):1822–30. doi: https://doi.org/10.1016/j.joca.2019.07.018.
[8] Safiri S, Kolahi A-A, Smith E, Hill C, Bettampadi D, Mansournia MA, et al. Global, regional and national burden of osteoarthritis 1990–2017: a systematic analysis of the Global Burden of Disease Study 2017. Ann Rheum Dis 2020;79(6):819–28. doi: https://doi.org/10.1136/annrheumdis-2019-216515.
[9] Moon PM, Shao ZY, Wambiekele G, Appleton CTG, Laird DW, Penuela S, et al. Global Deletion of Pannexin 3 Resulting in Accelerated Development of Aging-Induced Osteoarthritis in Mice. Arthritis & rheumatology (Hoboken, NJ) 2021;73(7):1178–88. doi: https://doi.org/10.1002/art.41651.
[10] Bao W-D, Pang P, Zhou X-T, Hu F, Xiong W, Chen K, et al. Loss of ferroportin induces memory impairment by promoting ferroptosis in Alzheimer's disease. Cell Death Differ 2021;28(5):1548–62. doi: https://doi.org/10.1038/s41418-020-00685-9.
[11] Chen X, Kang R, Kroemer G, Tang D. Broadening horizons: the role of ferroptosis in cancer. Nat Rev Clin Oncol 2021;18(5):280–96. doi: https://doi.org/10.1038/s41571-020-00462-0.
[12] Zhang Y, Swanda RV, Nie L, Liu X, Wang C, Lee H, et al. mTORC1 couples cyst(e)ine availability with GPX4 protein synthesis and ferroptosis regulation. Nat Commun 2021;12(1). doi: https://doi.org/10.1038/s41467-021-21841-w.
[13] Lei G, Mao C, Yan Y, Zhuang Li, Gan B. Ferroptosis, radiotherapy, and combination therapeutic strategies. Protein & cell 2021;12(11):836–57. doi: https://doi.org/10.1007/s13238-021-00841-y.
[14] Doll S, Freitas FP, Shah R, Aldrovandi M, da Silva MC, Ingold I, et al. FSP1 is a glutathione-independent ferroptosis suppressor. Nature 2019;575(7784):693–8. doi: https://doi.org/10.1038/s41586-019-1707-0.
[15] Bersuker K, Hendricks JM, Li Z, Magtanong L, Ford B, Tang PH, et al. The CoQ oxidoreductase FSP1 acts parallel to GPX4 to inhibit ferroptosis. Nature 2019;575(7784):688–92. doi: https://doi.org/10.1038/s41586-019-1705-2.
[16] Wei Z, Hao C, Huangfu J, Srinivasagan R, Zhang X, Fan X. Aging lens epithelium is susceptible to ferroptosis. Free Radic Biol Med 2021;167:94–108. doi: https://doi.org/10.1016/j.freeradbiomed.2021.02.010.
[17] Zhou R-P, Chen Y, Wei X, Yu B, Xiong Z-G, Lu C, et al. Novel insights into ferroptosis: Implications for age-related diseases. Theranostics 2020;10(26):11976–97. doi: https://doi.org/10.7150/thno.50663.
[18] Lin YC, Guo YR, Miyagi A, Levring J, MacKinnon R, Scheuring S. Force-induced conformational changes in PIEZO1. Nature 2019;573(7773):230–4. doi: https://doi.org/10.1038/s41586-019-1499-2.
[19] Eisenhoffer GT, Loftus PD, Yoshigi M, Otsuna H, Chien C-B, Morcos PA, et al. Crowding induces live cell extrusion to maintain homeostatic cell numbers in epithelia. Nature 2012;484(7395):546–9. doi: https://doi.org/10.1038/nature10999.
[20] Lee W, Nims RJ, Savadipour A, Zhang Q, Leddy HA, Liu F, et al. Inflammatory signaling sensitizes Piezo1 mechanotransduction in articular chondrocytes as a pathogenic feed-forward mechanism in osteoarthritis. Proc Natl Acad Sci USA 2021;118(13). doi: https://doi.org/10.1073/pnas.2001611118.
[21] Zhang G, Li X, Wu L, Qin YX. Piezo1 channel activation in response to mechanobiological acoustic radiation force in osteoblastic cells. Bone Res 2021;9(1):16. doi: https://doi.org/10.1038/s41413-020-00124-y.
[22] Baratchi S, Zaldivia MTK, Wallert M, Loseff-Silver J, Al-Aryahi S, Zamani J, et al. Transcatheter Aortic Valve Implantation Represents an Anti-Inflammatory Therapy Via Reduction of Shear Stress-Induced, Piezo-1-Mediated Monocyte

Activation. Circulation 2020;142(11):1092–105. doi: https://doi.org/10.1161/CIRCULATIONAHA.120.045536.
[23] Lee W, Leddy HA, Chen Y, Lee SH, Zelenski NA, McNulty AL, et al. Synergy between Piezo1 and Piezo2 channels confers high-strain mechanosensitivity to articular cartilage. PNAS 2014;111(47):E5114–22. doi: https://doi.org/10.1073/pnas.1414298111.
[24] Yuan H, Han Z, Chen Y, Qi F, Fang H, Guo Z, et al. Ferroptosis Photoinduced by New Cyclometalated Iridium(III) Complexes and Its Synergism with Apoptosis in Tumor Cell Inhibition. Angew Chem Int Ed Engl 2021;60(15):8174–81. doi: https://doi.org/10.1002/anie.202014959.
[25] Ricke KM, Pass T, Kimoloi S, Fahrmann K, Jungst C, Schauss A, et al. Mitochondrial Dysfunction Combined with High Calcium Load Leads to Impaired Antioxidant Defense Underlying the Selective Loss of Nigral Dopaminergic Neurons. J Neurosci 2020;40(9):1975–86. doi: https://doi.org/10.1523/JNEUROSCI.1345-19.2019.
[26] Srivastava N, Traynor D, Piel M, Kabla AJ, Kay RR. Pressure sensing through Piezo channels controls whether cells migrate with blebs or pseudopods. Proc Natl Acad Sci U S A 2020;117(5):2506–12. doi: https://doi.org/10.1073/pnas.1905730117.
[27] Wang D-W, Li S-J, Tan X-Y, Wang J-H, Hu Y, Tan Z, et al. Engineering of stepwise-targeting chitosan oligosaccharide conjugate for the treatment of acute kidney injury. Carbohydr Polym 2021;256:117556. doi: https://doi.org/10.1016/j.carbpol.2020.117556.
[28] Henke N, Albrecht P, Bouchachia I, Ryazantseva M, Knoll K, Lewerenz J, et al. The plasma membrane channel ORAI1 mediates detrimental calcium influx caused by endogenous oxidative stress. Cell Death Dis 2013;4. doi: https://doi.org/10.1038/cddis.2012.216.
[29] Tesoriere L, Attanzio A, Allegra M, Cilla A, Gentile C, Livrea M. Oxysterol mixture in hypercholesterolemia-relevant proportion causes oxidative stress-dependent eryptosis. Cell Physiol Biochem: Int J Exper Cell Physiol, Biochem, Pharmacol 2014;34(4):1075–89. doi: https://doi.org/10.1159/000366322.
[30] Katz JN, Arant KR, Loeser RF. Diagnosis and Treatment of Hip and Knee Osteoarthritis: A Review. JAMA 2021;325(6):568–78. doi: https://doi.org/10.1001/jama.2020.22171.
[31] Zhen G, Guo Q, Li Y, Wu C, Zhu S, Wang R, et al. Mechanical stress determines the configuration of TGFbeta activation in articular cartilage. Nat Commun 2021;12(1):1706. doi: https://doi.org/10.1038/s41467-021-21948-0.
[32] Coleman M, Ramakrishnan P, Brouillette M, Martin J. Injurious Loading of Articular Cartilage Compromises Chondrocyte Respiratory Function. Arthritis & rheumatology (Hoboken, NJ) 2016;68(3):662–71. doi: https://doi.org/10.1002/art.39460.
[33] Jeon J, Noh H-J, Lee H, Park H-H, Ha Y-J, Park SH, et al. TRIM24-RIP3 axis perturbation accelerates osteoarthritis pathogenesis. Ann Rheum Dis 2020;79(12):1635–43. doi: https://doi.org/10.1136/annrheumdis-2020-217904.
[34] Wu Y, Zhang S, Gong X, Tam S, Xiao D, Liu S, et al. The epigenetic regulators and metabolic changes in ferroptosis-associated cancer progression. Mol Cancer 2020;19(1):39. doi: https://doi.org/10.1186/s12943-020-01157-x.
[35] Proneth B, Conrad M. Ferroptosis and necroinflammation, a yet poorly explored link. Cell Death Differ 2019;26(1):14–24. doi: https://doi.org/10.1038/s41418-018-0173-9.
[36] Bomer N, Cornelis FMF, Ramos YFM, den Hollander W, Storms L, van der Breggen R, et al. The effect of forced exercise on knee joints in Dio2(-/-) mice: type II iodothyronine deiodinase-deficient mice are less prone to develop OA-like cartilage damage upon excessive mechanical stress. Ann Rheum Dis 2016;75(3):571–7. doi: https://doi.org/10.1136/annrheumdis-2014-206608.
[37] Zheng J, Conrad M. The Metabolic Underpinnings of Ferroptosis. Cell Metab 2020;32(6):920–37. doi: https://doi.org/10.1016/j.cmet.2020.10.011.
[38] Mao C, Liu X, Zhang Y, Lei G, Yan Y, Lee H, et al. DHODH-mediated ferroptosis defence is a targetable vulnerability in cancer. Nature 2021;593(7860):586–90. doi: https://doi.org/10.1038/s41586-021-03539-7.
[39] Gudipaty SA, Lindblom J, Loftus PD, Redd MJ, Edes K, Davey CF, et al. Mechanical stretch triggers rapid epithelial cell division through Piezo1. Nature 2017;543(7643):118–21. doi: https://doi.org/10.1038/nature21407.
[40] Swain SM, Romac JM, Shahid RA, Pandol SJ, Liedtke W, Vigna SR, et al. TRPV4 channel opening mediates pressure-induced pancreatitis initiated by Piezo1 activation. J Clin Invest 2020;130(5):2527–41. doi: https://doi.org/10.1172/JCI134111.
[41] Liang G-P, Xu J, Cao L-l, Zeng Y-H, Chen B-X, Yang J, et al. Piezo1 induced apoptosis of type II pneumocytes during ARDS. Respir Res 2019;20(1). doi: https://doi.org/10.1186/s12931-019-1083-1.
[42] Blagojevic M, Camilli G, Maxson M, Hube B, Moyes DL, Richardson JP, et al. Candidalysin triggers epithelial cellular stresses that induce necrotic death. Cell Microbiol 2021;23(10). doi: https://doi.org/10.1111/cmi.v23.1010.1111/cmi.13371.
[43] Okazaki T, Tanaka Y, Nishio R, Mitsuiye T, Mizoguchi A, Wang J, et al. Autoantibodies against cardiac troponin I are responsible for dilated cardiomyopathy in PD-1-deficient mice. Nat Med 2003;9(12):1477–83. doi: https://doi.org/10.1038/nm955.
[44] Zhong G, Long H, Chen F, Yu Y. Oxoglaucine mediates Ca(2+) influx and activates autophagy to alleviate osteoarthritis through the TRPV5/calmodulin/CAMK-II pathway. Br J Pharmacol 2021;178(15):2931–47. doi: https://doi.org/10.1111/bph.15466.
[45] Wang Y, Xiang C, Sun X, Wu S, Lv J, Li P, et al. DAla2GIP antagonizes H2O2-induced chondrocyte apoptosis and inflammatory factor secretion. Bone 2019;127:656–63. doi: https://doi.org/10.1016/j.bone.2019.05.026.
[46] Wu F, Chi Y, Jiang Z, Xu Y, Xie L, Huang F, et al. Hydrogen peroxide sensor HPCA1 is an LRR receptor kinase in Arabidopsis. Nature 2020;578(7796):577–81. doi: https://doi.org/10.1038/s41586-020-2032-3.
[47] Jia H, Ma X, Wei Y, Tong W, Tower RJ, Chandra A, et al. Loading-Induced Reduction in Sclerostin as a Mechanism of Subchondral Bone Plate Sclerosis in Mouse Knee Joints During Late-Stage Osteoarthritis. Arthrit Rheumatol (Hoboken, NJ) 2018;70(2):230–41. doi: https://doi.org/10.1002/art.40351.
[48] Christiansen L, Morsing M, Reimann M, Martinussen T, Birlie Z, Schou-Pedersen A, et al. Pharmacokinetics of Repeated Oral Dosing with Coenzyme Q10 in Cavalier King Charles Spaniels with Myxomatous Mitral Valve Disease. Antioxidants (Basel, Switzerland) 2020;9. doi: https://doi.org/10.3390/antiox909082.
[49] Zhao Y, Liu B, Tian Q, Wei J, Richbourgh B, Liu C. Progranulin protects against osteoarthritis through interacting with TNF-α and β-Catenin signalling. Ann Rheum Dis 2015;74(12):2244–53. doi: https://doi.org/10.1136/annrheumdis-2014-205779.
[50] Stegen S, Laperre K, Eelen G, Rinaldi G, Fraisl P, Torrekens S, et al. HIF-1α metabolically controls collagen synthesis and modification in chondrocytes. Nature 2019;565(7740):511–5. doi: https://doi.org/10.1038/s41586-019-0874-3.
[51] Mannes AM, Seiler A, Bosello V, Maiorino M, Conrad M. Cysteine mutant of mammalian GPx4 rescues cell death induced by disruption of the wild-type selenoenzyme. FASEB J: Offic Publ Feder Am Societ Exper Biol 2011;25(7):2135–44. doi: https://doi.org/10.1096/fj.10-177147.